

## Structure and magnetic properties of the cubic oxide fluoride BaFeO<sub>2</sub>F

Berry, Frank; Coomer, FC; Hancock, Cathryn; Helgason, O; Moore, EA; Slater, Peter; Wright, Adrian; Thomas, MF

DOI:

[10.1016/j.jssc.2011.04.011](https://doi.org/10.1016/j.jssc.2011.04.011)

*Citation for published version (Harvard):*

Berry, F, Coomer, FC, Hancock, C, Helgason, O, Moore, EA, Slater, P, Wright, A & Thomas, MF 2011, 'Structure and magnetic properties of the cubic oxide fluoride BaFeO<sub>2</sub>F', *Journal of Solid State Chemistry*, vol. 184, no. 6, pp. 1361-1366. <https://doi.org/10.1016/j.jssc.2011.04.011>

[Link to publication on Research at Birmingham portal](#)

### General rights

Unless a licence is specified above, all rights (including copyright and moral rights) in this document are retained by the authors and/or the copyright holders. The express permission of the copyright holder must be obtained for any use of this material other than for purposes permitted by law.

- Users may freely distribute the URL that is used to identify this publication.
- Users may download and/or print one copy of the publication from the University of Birmingham research portal for the purpose of private study or non-commercial research.
- User may use extracts from the document in line with the concept of 'fair dealing' under the Copyright, Designs and Patents Act 1988 (?)
- Users may not further distribute the material nor use it for the purposes of commercial gain.

Where a licence is displayed above, please note the terms and conditions of the licence govern your use of this document.

When citing, please reference the published version.

### Take down policy

While the University of Birmingham exercises care and attention in making items available there are rare occasions when an item has been uploaded in error or has been deemed to be commercially or otherwise sensitive.

If you believe that this is the case for this document, please contact [UBIRA@lists.bham.ac.uk](mailto:UBIRA@lists.bham.ac.uk) providing details and we will remove access to the work immediately and investigate.

**Structure and magnetic properties of the cubic oxide fluoride BaFeO<sub>2</sub>F**

**Frank J Berry,<sup>1,2</sup> Fiona C Coomer,<sup>1</sup> Cathryn Hancock,<sup>1</sup> Örn Helgason,<sup>3</sup> Elaine A Moore,<sup>2</sup> Peter R Slater,<sup>1</sup> Adrian J Wright<sup>1</sup> and Michael F Thomas<sup>4</sup>**

<sup>1</sup> *School of Chemistry, The University of Birmingham, Edgbaston, Birmingham B15 2TT, UK*

<sup>2</sup> *Department of Chemistry, The Open University, Walton Hall, Milton Keynes MK7 6AA, UK*

<sup>3</sup> *Science Institute, University of Iceland, Dunhagi 3, IS-107 Reykjavik, Iceland*

<sup>4</sup> *Department of Physics, The University of Liverpool, Liverpool L69 3BX, UK*

**Submitted to: J Solid State Chemistry**

**Correspondence to: Professor Frank Berry**

**School of Chemistry  
The University of Birmingham  
Edgbaston  
Birmingham B15 2TT  
UK**

**Email: [f.j.berry.1@bham.ac.uk](mailto:f.j.berry.1@bham.ac.uk)**

## Abstract

Fluorination of the parent oxide,  $\text{BaFeO}_{3-\delta}$ , with polyvinylidene fluoride gives rise to a cubic compound with  $a = 4.0603(4) \text{ \AA}$  at 298K.  $^{57}\text{Fe}$  Mössbauer spectra confirmed that all the iron is present as  $\text{Fe}^{3+}$ . Neutron diffraction data showed complete occupancy of the anion sites indicating a composition  $\text{BaFeO}_2\text{F}$ , with a large displacement of the iron off-site. The magnetic ordering temperature was determined as  $T_N = 645 \pm 5\text{K}$ . Neutron diffraction data at 4.2K established G-type antiferromagnetism with a magnetic moment per  $\text{Fe}^{3+}$  ion of  $3.95\mu_B$ . However, magnetisation measurements indicated the presence of a weak ferromagnetic moment which is assigned to the canting of the antiferromagnetic structure.  $^{57}\text{Fe}$  Mössbauer spectra in the temperature range 10 to 300K were fitted with a model of fluoride ion distribution that retains charge neutrality of the perovskite unit cell.

Keywords:  $\text{BaFeO}_2\text{F}$ ; oxide fluoride; canted antiferromagnet

## 1. Introduction

The identification of superconductivity in oxide fluorides of composition  $\text{Sr}_2\text{CuO}_2\text{F}_{2+x}$  which adopt a perovskite-related structure has generated considerable activity in the synthesis and characterisation of new inorganic oxide fluorides with related structures [1-3]. We have recently reported [4, 5] on the fluorination of oxygen-deficient perovskite-related  $\text{SrFeO}_{3-\delta}$  to give a compound of composition  $\text{SrFeO}_2\text{F}$  with a cubic unit cell and have formulated a model related to the pattern of substitution by fluorine on the octahedral arrangement of oxygen sites around iron in which  $\text{SrFeO}_2\text{F}$  undergoes a magnetic transition around 300K from a low temperature state with random spin directions to an antiferromagnetic state. We have also prepared the related cubic phase of composition  $\text{BaFeO}_2\text{F}$  and, in a preliminary neutron powder diffraction study, found it to exhibit G-type antiferromagnetic order at 298K [6]. However, this preliminary study [6] generated significant questions which required further detailed investigation. For example, the high thermal displacement parameter ( $3.6\text{\AA}^2$ ) for the iron site suggests the possibility of a series of random displacements. However, the fact that the sample possesses cubic symmetry implies that if such displacements are present there is no unique direction for them which raises the question of whether, at lower temperatures, a phase transition to a non-centrosymmetric ferroelectric cell may occur leading to the co-existence of magnetic- and ferroelectric- order. In order to address these matters we have recorded neutron powder diffraction data at 4.2K and, in order to investigate further the magnetic properties of the material, have recorded DC susceptibility measurements between 5 and 300K and field-dependent DC measurements at 5K between 0 and 7T together with Mossbauer spectra between 300 and 10K. We have also performed calculations to explore the displacement of iron and magnetic interactions within the material.

Hence we now report here on an examination of the structural and magnetic properties of cubic  $\text{BaFeO}_2\text{F}$  between 4.2 and 650K which modifies the preliminary description of the material [6] and shows it to be substantially different from  $\text{SrFeO}_2\text{F}$ .

## 2. Experimental

The oxygen deficient  $\text{BaFeO}_{3-\delta}$  was prepared by the calcination of appropriate quantities of a well ground mixture of barium(II) carbonate and iron(III) oxide at 1100 °C for 24

hours in air with intermediate regrinding. Fluorination was achieved by mixing the  $\text{BaFeO}_{3-\delta}$  phase with polyvinylidene fluoride in a 1 : 0.60 molar ratio (precursor oxide : monomer unit) [7] and heating this mixture at  $375^\circ\text{C}$  for 24 hours in air in a furnace within a fume cupboard.

X-ray powder diffraction patterns were recorded with a Panalytical X'Pert Pro diffractometer using  $\text{Cu K}\alpha$  radiation at 298K. Neutron diffraction data were collected at 4.2K on the POLARIS diffractometer, ISIS, Rutherford Appleton Laboratory. All structure refinements used the GSAS suite of the Rietveld refinement software [8].

DC susceptibility measurements were performed over the temperature range 5 to 300K using a Quantum Design MPMS SQUID magnetometer. The samples were pre-cooled to 5K in zero field (ZFC) and also in an applied field of 0.1T (FC) and values of  $\chi$  measured whilst warming in a field of 0.1T. Field-dependent DC susceptibility measurements were performed with a Quantum Design PPMS system with the ACMS control system in DC extraction mode. Measurements were performed at 5K between 0 and 7T.

The  $^{57}\text{Fe}$  Mössbauer spectra were recorded between 10 and 650K with a constant acceleration spectrometer using a Co/Rh source of *ca.* 25 mCi. The spectra between 10 and 300K were recorded with a liquid helium flow cryostat and spectra between 400 and 650K were recorded *in situ* using a specially designed furnace [9]. The  $^{57}\text{Fe}$  Mössbauer chemical isomer shift data are quoted relative to metallic iron at room temperature.

Calculations were performed using CRYSTAL06 [10] on  $2\times 2\times 2$  supercells of cubic  $\text{BaFeO}_2\text{F}$  using the experimental cell dimensions. Such a supercell permits exploration of the different types of antiferromagnetism. The basis sets used were all electron sets on Fe {8-6411-d41} [11], O {8-411-d1} [12] and F {7-311} [13]. A pseudopotential basis set [14] was used for Ba to reduce the computer resource needed. The hybrid functional B3LYP was used as it has been shown that methods beyond DFT such as hybrid functionals and DFT+U are needed for the correct description of solids with highly correlated cations. Supercells with the iron ions surrounded by four oxide and two fluoride ions with the fluoride ions arranged trans or cis were used. Ferromagnetic and A-, C- and G- type antiferromagnetic spin arrangements were explored for the lowest energy configuration.

### 3. Results and Discussion

### 3.1 X-ray and neutron powder diffraction

The X-ray powder diffraction pattern recorded from BaFeO<sub>2</sub>F at 298K indicated a cubic phase with unit cell size,  $a = 4.0603(4)$  Å. The structure of this phase was previously examined by neutron diffraction at 298K and 773K [6] and confirmed cubic symmetry and indicated G-type antiferromagnetic order at the former temperature. However, as noted earlier, the work suggested some displacement of the iron [6]. In an extension of this work, we have now analysed the structure at low temperature (4.2K) to determine if there is a lowering of symmetry and hence a phase transition to a non-centrosymmetric unit cell. The low temperature data showed very little change from the room temperature data, with a cubic cell and magnetic (G-type antiferromagnet) ordering. Calculations supported the G-type antiferromagnetic cell as the lowest energy ordering at low temperature if spin-orbit coupling is neglected. The refined structural parameters are given in Table 1 with selected bond distances in Table 2, and the neutron diffraction profiles are shown in Figure 1. The results show that, as in the case of the room temperature data, there remains a high thermal displacement parameter for the iron, indicating some off centre displacement. The fact that the cell symmetry is cubic means that there is no unique long range direction for these displacements. Instead there are likely to be local displacements which may be influenced by both the large size of barium, which leads to underbonding at the B cation site, and the mixed occupation of anion sites by F<sup>-</sup> and O<sup>2-</sup> ions. To illustrate the underbonding at the iron site, bond valence calculations showed that for a Fe(III)O<sub>4</sub>F<sub>2</sub> octahedron, the bond valence sum (BVS) is 2.76.

The potential effect of the O/F distribution can be considered as follows. The charge neutral perovskite unit cell contains four O<sup>2-</sup> and two F<sup>-</sup> ions. Random occupation of the six anion sites gives cis or trans configurations in a ratio of 4:1. The Coulomb attraction between O<sup>2-</sup> and Fe<sup>3+</sup> ions is twice that between F<sup>-</sup> and Fe<sup>3+</sup> ions because of the double negative charge on the O<sup>2-</sup> ion. However, the core size of the F<sup>-</sup> ion will be less than that of the O<sup>2-</sup> ion because of the greater nuclear charge, 9(F) as opposed to 8(O). In ionic bonding these Coulomb attraction and core repulsion terms act in opposition. While detailed calculations would be required to determine quantitatively the net effect it is easily appreciated that the ionic bonding along a line O<sup>2-</sup> - Fe<sup>3+</sup> - F<sup>-</sup> should be unbalanced

leading to a displacement of the  $\text{Fe}^{3+}$  ion. In the trans configuration there would be predicted to be no net displacement of the  $\text{Fe}^{3+}$  ion as in all directions the opposite forces are balanced but in the cis configuration displacements of the  $\text{Fe}^{3+}$  ion will be predicted to occur. An indication of the effect of  $\text{O}^{2-}$ ,  $\text{F}^-$  distribution on iron displacement is provided by periodic ab initio calculations on a structure in which all  $\text{Fe}^{3+}$  ions adopt the cis configuration. Optimisation of the atomic positions within the cell leads to a displacement of the  $\text{Fe}^{3+}$  ion towards the  $\text{O}^{2-}$  ions trans to the  $\text{F}^-$ . The calculations suggest displacement along the F-Fe-F angle bisector with Fe-O distances of 1.91Å (for  $\text{O}^{2-}$  opposite  $\text{F}^-$ ) and 2.05Å, and an Fe-F distance of 2.17Å. If the  $\text{F}^-$  ions are randomly distributed (consistent with the neutral cell) the calculations would suggest that  $\text{Fe}^{3+}$  displacement will occur along all possible directions of these bisectors.

In order to investigate experimentally the direction of the displacements, the neutron diffraction data were re-examined and the iron allowed to move off site. Interestingly, rather than a displacement along the bond angle bisector, a different displacement direction was observed with the experimental data being best fitted by moving the iron off the ideal 1b (1/2, 1/2, 1/2) site to the 6f (x, 1/2, 1/2) site with 1/6 occupancy. This refinement gave a stable position at (0.4386(3), 1/2, 1/2) with the atomic displacement parameter ( $U_1(\times 100)$ ) reducing to 0.38 Å<sup>2</sup> and with a small improvement in the fit (Tables 3 and 4). This refinement therefore suggests an average shift of the iron off site of *ca.*0.25 Å directly along the Fe-O/F bond axis. Such a displacement is typical of ferroelectric-type displacements observed in perovskites such as  $\text{BaTiO}_3$  and would suggest that local ferroelectric-type displacements are dominant as opposed to the effect of the local distribution of O/F examined by the modeling studies. The origin for this displacement is the large size of Ba leading to underbonding at the iron site, as highlighted above.

**Table 1.** Refined structural parameters for  $\text{BaFeO}_2\text{F}$  at 4K (no Fe displacement)

Atom	Site	x	y	z	$U_1(\times 100)/\text{Å}^2$	Site Occupancy
Ba	1a	0	0	0	0.08(1)	1
Fe	1b	0.5	0.5	0.5	2.99(2)	1
O/F	3c	0.5	0.5	0	0.461(8)	1

$Pm-3m$ ,  $a = 4.0447(1) \text{ \AA}$ ,  $\chi^2 = 3.16$ ,  $R_{wp} = 0.0138$ ,  $R_p = 0.0222$   
 Fe magnetic moment =  $3.94(4) \mu_B$

**Table 2.** Selected bond distances for BaFeO<sub>2</sub>F at 4K (no Fe displacement)

Bond	Bond Distance/ $\text{\AA}$
Fe-O/F	2.0224 (1) (x 6)
Ba-O/F	2.8601 (1) (x 12)

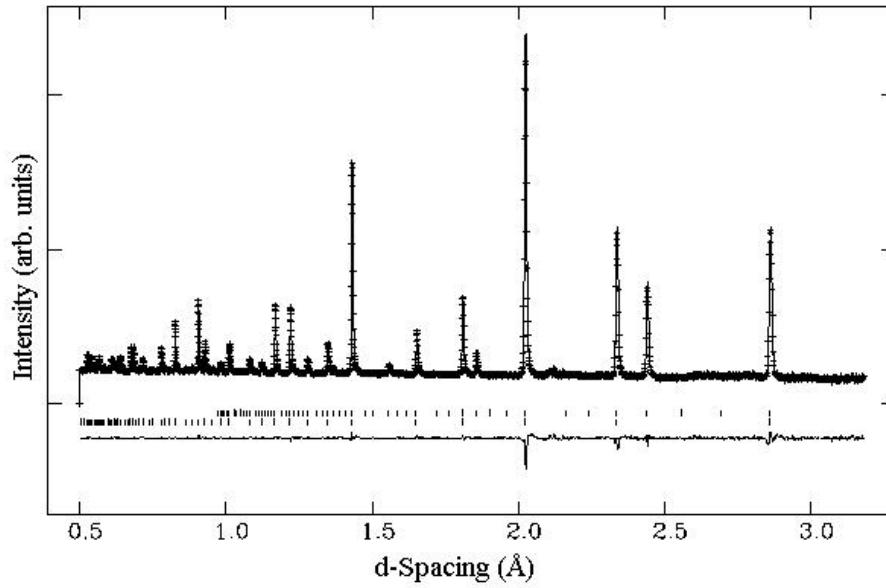


**Fig. 1.** Observed, calculated and difference neutron powder diffraction profiles for BaFeO<sub>2</sub>F at 4.2K (the lower tick marks are the crystallographic structure reflections; the upper tick marks are the magnetic structure reflections).

**Table 3.** Refined structural parameters for BaFeO<sub>2</sub>F at 4K (with Fe displacement)

Atom	Site	x	y	z	$U_1(\times 100)\text{\AA}^2$	Site Occupancy
Ba	1a	0	0	0	0.08(1)	1
Fe	6e	0.4386 (3)	0.5	0.5	0.38(3)	0.167
O/F	3c	0.5	0.5	0	0.464(7)	1

$Pm-3m$ ,  $a = 4.0447(1) \text{ \AA}$ ,  $\chi^2 = 2.79$ ,  $R_{wp} = 0.0130$ ,  $R_p = 0.0224$   
 Fe magnetic moment =  $3.99(4) \mu_B$



**Table 4.** Selected bond distances for BaFeO<sub>2</sub>F at 4K (with Fe displacement)

Bond	Bond Distance/ Å
Fe-O/F	2.0376 (2) (x4)
Fe-O/F	1.774 (1) (x1)
Fe-O/F	2.271 (1) (x1)
Ba-O/F	2.8601 (1) (x12)

### 3.2 Magnetisation

The variation of magnetic susceptibility  $\chi$  (in an applied field of 0.1T) with increasing temperature from 5 to 300K following pre-cooling in (i) zero applied field (ZFC) and (ii) an applied field of 0.1T (FC) is shown in Figure 2.

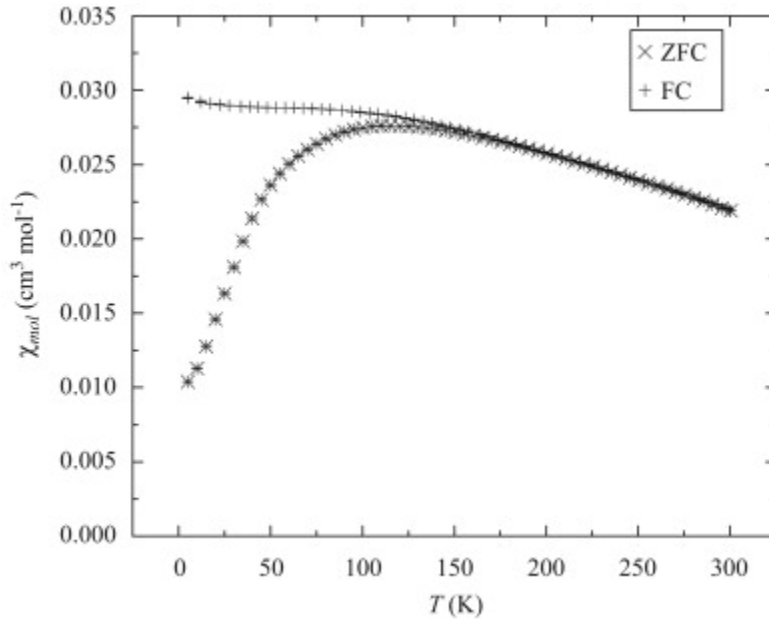
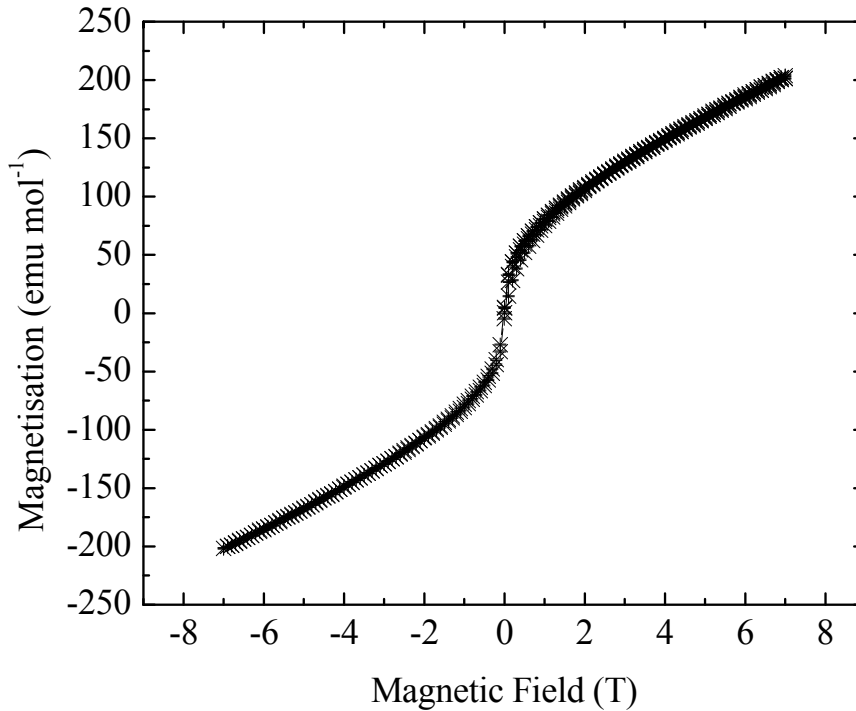


Figure 2 Variation of magnetisation between 5 and 300K. The data were recorded at increasing temperature in a measuring field of 0.1T. Separate plots show field cooled (FC) and zero field cooled (ZFC) data.

It is evident for  $T < 150\text{K}$  that there is a divergence in susceptibility data between zero field cooled (ZFC) samples and those cooled in an applied field of 0.1T (FC). At temperatures above 150K the data coincide and show a gentle decrease with increase in temperature. This behaviour modifies the picture of a pure G-type antiferromagnetic structure by indicating a weak ferromagnetic component.

The variation of magnetisation  $M$  in a field sweep measurement at 5K is shown in Figure 3.



**Fig. 3.** Field dependent magnetization measured at 5K.

It is seen that an increasing  $|H|$  causes a relatively rapid increase in  $|M|$  up to a value of  $H \sim 0.2\text{T}$  whereupon there is a change of slope to one proportional to the increasing  $H$ . The shape of this  $M$  vs  $H$  plot is characteristic of weak ferromagnetism where the steep initial slope arises from the saturation of the weak ferromagnetic component.

The magnitude of the weak moment was estimated by extrapolating a linear fit of the data in the range  $4.5\text{T} \leq H \leq 7\text{T}$  to  $0\text{T}$  and measuring the intercept on the  $M$  axis. This results in a value of  $M = 80 \pm 1 \text{ emu.mol}^{-1}$  equivalent to a moment per  $\text{Fe}^{3+}$  ion of  $0.01\mu_{\text{B}}$ .

Comparing this value with the  $\text{Fe}^{3+}$  moment of  $3.95\mu_{\text{B}}$  equates to a canting angle, estimated by trigonometry from  $\sin^{-1}(0.01/3.95)$ , of  $0.16 \pm 0.02^\circ$ .

### 3.2.1 Magnetisation results – the case for a weak ferromagnet

Neutron diffraction confirms that the basic magnetic structure of the  $\text{Fe}^{3+}$  moments is of a

G-type antiferromagnet, but features of the susceptibility ( $\chi$ ) vs temperature (T) plot (Figure 2), particularly the divergence between ZFC and FC below *ca.* 150K, suggest that a more complex description is necessary. By considering the presence of canting of the antiferromagnetic moments below *ca.* 150K, it is possible to reconcile the appearance of the susceptibility data with the neutron diffraction-determined magnetic structure. From the hysteresis data in Figure 3 the magnitude of the weak ferromagnetic moment at 5K has been evaluated as  $0.01\mu\text{B}$  per  $\text{Fe}^{3+}$  ion suggesting a small canting angle of  $0.16\pm 0.02^\circ$ , which would not be discernible *via* neutron diffraction.

Although we cannot exclude the possibility of the presence of separate magnetic impurities below the limit of detectability of the techniques used here we contend that the results, taken together and including the apparent continuous nature of the susceptibility data, supports our above interpretation in terms of a canted structure for the oxide fluoride.

### 3.3 *Mössbauer spectroscopy*

The  $^{57}\text{Fe}$  Mössbauer spectra recorded between 10 and 300K are shown in Figure 4 and those recorded between 400 and 650K are collected in Figure 5. Representative  $^{57}\text{Fe}$  Mössbauer parameters from Figures 4 and 5 are collected in Table 5.

The Table contains parameters for two different fitting procedures. The spectra from 10 to 300K were fitted with components with parameters partly determined by a model of the perovskite cell containing four  $\text{O}^{2-}$  and two  $\text{F}^-$  ions. The spectra from 400 to 650K were fitted with phenomenological components to obtain the magnetic ordering temperature. Isomer shift values are quoted relative to metallic iron at 298K

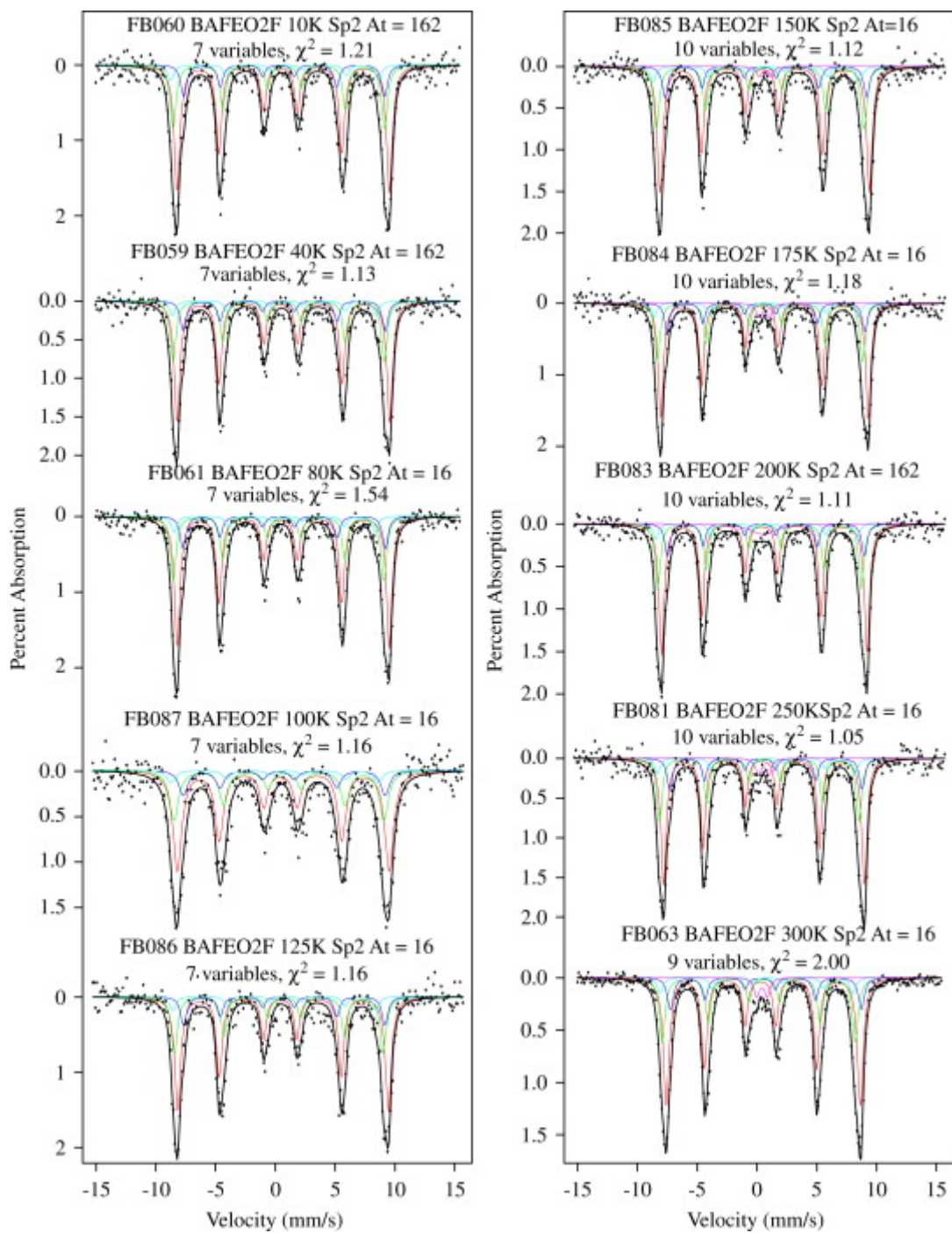


Figure 4  $^{57}\text{Fe}$  Mössbauer spectra recorded from  $\text{BaFeO}_2\text{F}$  between 10 and 300K. The spectra were fitted with components constrained by a model of  $\text{F}^-$  distribution in which the unit perovskite cell contains four  $\text{O}^{2-}$  and two  $\text{F}^-$  ions.

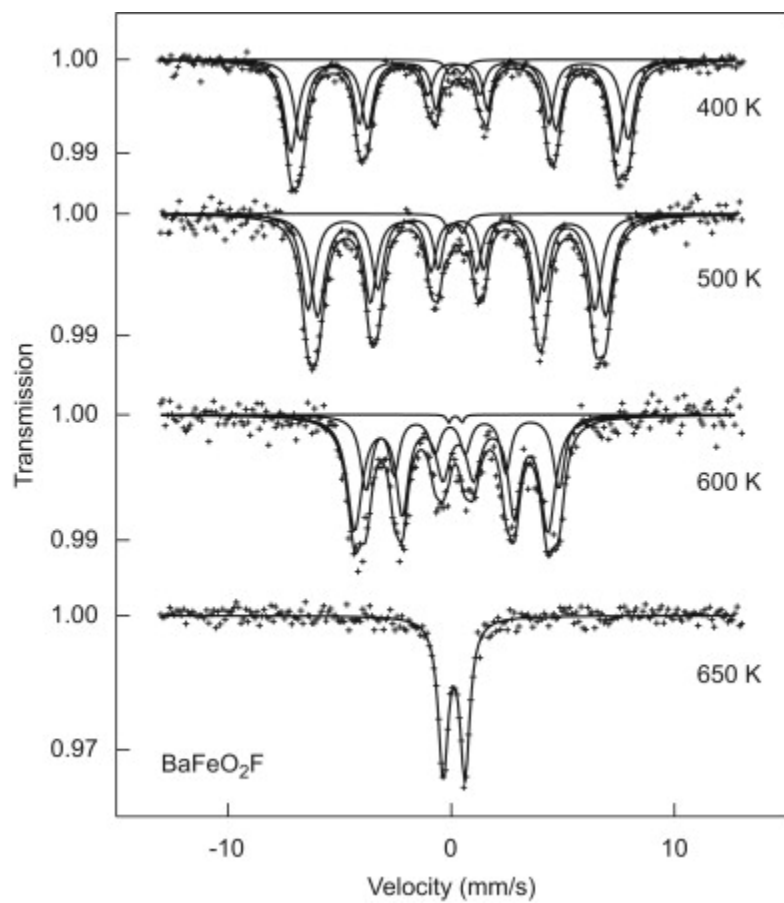


Figure 5  $^{57}\text{Fe}$  Mössbauer spectra recorded from BaFeO<sub>2</sub>F between 400 and 650K. The spectra were fitted with phenomenological components to measure the magnetic ordering temperature.

**Table 5.** Fitting parameters for the  $^{57}\text{Fe}$  Mössbauer spectra.

Temperature (K)	Isomer shift (mm/s)	Quadrupole Interaction (mm/s)	Line Width (mm/s)	Hyperfine Field (kG)	Relative Area (%)
10	0.54	0.24	0.56	550	53.3
	0.53	-0.46	0.56	548	26.7
	0.50	0.48	0.56	522	13.3
	0.41	-0.66	0.56	541	6.7
80	0.55	0.24	0.56	549	53.3
	0.49	-0.46	0.56	545	26.7
	0.50	0.48	0.56	524	13.3
	0.42	-0.96	0.56	521	6.7
150	0.52	0.24	0.54	543	52.3
	0.49	-0.46	0.54	538	26.1
	0.50	0.48	0.54	522	13.1
	0.42	-0.96	0.54	535	6.5
	0.66	1.00	0.56	0	2.0
300	0.40	0.24	0.55	503	51.4
	0.37	-0.46	0.55	501	25.7
	0.50	0.48	0.55	495	12.9
	0.42	-0.96	0.55	499	6.4
	0.40	0.88	0.56	0	3.6
400	0.32	0.01		452	77
	0.37	0.01		479	21
	0.22	0.62		0	2
500	0.27	-0.03		384	54
	0.24	0.01		413	44
	0.17	0.74		0	2
600 <sup>†</sup>	0.17	0.01		258	73
	0.23	-0.03		288	27
650	0.13	0.96		0	100

<sup>†</sup> The quadrupole split absorption equated to less than 1% of the spectral area at 600K

There are two features of the results presented in Figures 4 and 5 and in Table 5 which are readily amenable to interpretation. Firstly, all the spectral components have chemical isomer shifts characteristic of the presence of  $\text{Fe}^{3+}$  ions which, together with the presence of  $\text{Ba}^{2+}$ ,  $\text{O}^{2-}$  and  $\text{F}^-$  and the neutron diffraction data showing complete occupancy of the anion sites is consistent with the formulation  $\text{BaFeO}_2\text{F}$ . Secondly, the spectra recorded at temperatures exceeding 400K in Figure 5 show decreasing magnitudes of magnetic hyperfine field until, at 650K, the magnetic hyperfine field collapses to a quadrupole split doublet indicative of the paramagnetic state. The variation of the average magnetic hyperfine field with increasing temperature is shown in Figure 6 and, from

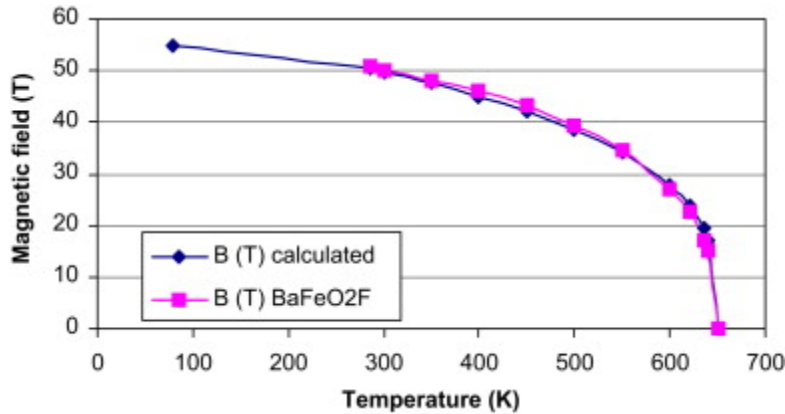


Figure 6 Variation of the magnetic hyperfine field in  $\text{BaFeO}_2\text{F}$  with temperature.

The values of hyperfine field are taken from the spectra shown in Figure 5.

these data, a magnetic ordering temperature for  $\text{BaFeO}_2\text{F}$  of  $645 \pm 5\text{K}$  can be deduced. This is lower than the magnetic ordering temperature of  $685 \pm 5\text{K}$  which was previously found for  $\text{SrFeO}_2\text{F}$  [5]. The variation of the average magnetic hyperfine field with increasing temperature is also compared in Figure 6 with that calculated from the expression  $B = B_0 (1 - T/T_C)^\beta$ , where  $B$  is the magnetic hyperfine field,  $B_0$  is the magnetic hyperfine field at 0K,  $T_C$  is the magnetic ordering temperature, and  $\beta$  is usually in the range of 0.25 – 0.33 and, in this calculation, was taken as 0.3. The results displayed in Figure 6 show good agreement between the experimentally determined data and those predicted theoretically.

The  $^{57}\text{Fe}$  Mössbauer spectra recorded between 10 and 300K were analysed to test a model

for the random occupation by fluorine of anion sites. This model assumes a charge neutral perovskite-related unit cell with four  $O^{2-}$  and two  $F^-$  anions. Spatially the two  $F^-$  anions can be in cis or trans arrangements with relative frequencies of 4:1 for a purely random occupation in the iron coordination sphere. The principal axes of the electric field gradients (EFG) are taken to be along the directions of maximum symmetry in each case (parallel to the  $F^-$  trans direction and along the direction of the bisector of the two  $F^-$  anions in the case of the cis arrangement). The hyperfine field is assumed to be parallel to a cube edge as in most antiferromagnetic perovskite-related structures. This model gives rise to four magnetic sextet components – two arising from the cis arrangement with the hyperfine field making angles of  $45^\circ$  and  $90^\circ$  with the EFG in an intensity ratio of 2:1 and two from the trans arrangement with the hyperfine field making angles of  $90^\circ$  and  $0^\circ$  to the EFG with an intensity ratio of 2:1. Thus the fitting area ratios were initially fixed as 8:4:2:1 respectively, with subsequent refinement leading to negligible change in these ratios, confirming the random arrangement. The magnitude of the quadrupole interaction is fixed at the value of  $0.96\text{mms}^{-1}$  from the doublet measured at 650K. This magnitude is taken for cis and trans sites but in the magnetically split spectra a choice of sign remains which was determined by fitting to be positive for cis and negative for trans sites. The angles between the hyperfine field and quadrupole interaction are specified as above. The variable parameters are isomer shift and hyperfine field values and a representative selection of these parameters are listed in Table 5. The results show that good fits were obtained with this fitting method for temperatures up to  $\sim 150\text{K}$ . Above this temperature a non-magnetic component with relative intensity  $\sim 3\%$  is also required. Nevertheless the good fit of the majority magnetic spectrum gives confidence in the model of  $F^-$  distribution that gives a charge neutral perovskite-related unit cell, with a random arrangement of  $F^-$  anions.

#### **4. Conclusions**

The cubic oxide fluoride  $\text{BaFeO}_2\text{F}$  is substantially different from the related phase of composition  $\text{SrFeO}_2\text{F}$ . The main magnetic features observed here concerning the magnetic properties of  $\text{BaFeO}_2\text{F}$  are

(i) The variation of magnetic hyperfine field with temperature which establishes a



magnetic ordering temperature of  $T_N = 645 \pm 5 \text{K}$ .

(ii) Neutron diffraction measurements down to 5K which establish that the  $\text{Fe}^{3+}$  moments are ordered in a G-type antiferromagnetic structure.

(iii) The magnetisation results which modify the picture of a pure G-type antiferromagnet introducing evidence of a weak ferromagnetic structure with canting of the moments by  $\sim 0.16^\circ$  to give a weak ferromagnetic moment of  $\sim 0.01 \mu_B$  per  $\text{Fe}^{3+}$  ion.

(iv) The large mean square displacement of the  $\text{Fe}^{3+}$  ions down to 5K in the neutron diffraction data with further refinements suggesting an average  $0.25 \text{\AA}$  shift off-site.

### **Acknowledgements.**

MFT acknowledges EPSRC support for the low temperature Mössbauer spectroscopy. We thank EPSRC for funding (studentship for CH), ISIS, Rutherford Appleton Laboratory for the provision of neutron diffraction beam time, and Ron Smith for help with the collection of neutron diffraction data and EAM acknowledges The Open University Science Faculty support for the Linux Beowulf cluster.

### **References**

- [1] M.G. Francesconi, C. Greaves, Supercond. Sci. Technol. 10 (1997) A29
- [2] C. Greaves, M.G. Francesconi, Curr. Opin. Solid State Mater. Sci. 3 (1998) 132
- [3] E.E. McCabe, C. Greaves, J. Fluorine Chem. 128 (2007) 448
- [4] F.J. Berry, X. Ren, R. Heap, P.R. Slater, M.F. Thomas, Solid State Commun. 134 (2005) 621
- [5] F.J. Berry, R. Heap, O. Helgason, E.A. Moore, S. Shim, P.R. Slater, M.F. Thomas, J. Phys. : Cond. Matter. 20 (2008) 215207
- [6] R. Heap, P.R. Slater, F.J. Berry, O. Helgason, A.J. Wright, Solid State Commun. 141 (2007) 476
- [7] P.R. Slater, J. Fluorine Chem. 117 (2002) 43
- [8] A.C. Larson, R.B. Von Dreele, Los Alamos National Laboratory, Report No LA-UR-96-748 (1987)
- [9] O. Helgason, H.P. Gunnlaugsson, K. Jonsson, S. Steinhörsson, Hyperfine Interact. 91 (1994) 59

- [10] R. Dovesi, V.R. Saunders, C. Roetti, R.Orlando, C.M. Zieovich-Wilson, F. Pascale, B.Civalleri, K.Doll, N.M.Harrison, L.J.Bush, Ph.D'Arco, M.Llunell, *CRYSTAL06 User's Manual*, University of Torino, Torino(2006)
- [11] M. Catti, G. Valerio, R. Dovesi, Phys. Rev.B 51 (1995) 7441
- [12] M. Catti, G. Sandrone, G. Valerio, R. Dovesi , J.Phys.Chem.Solids 57 (1996) 1735
- [13] J.M. Ricart, R. Dovesi, C. Roetti, V.R. Saunders, Phys.Rev.B 52 (1995) 2381
- [14] S. Piskunov, E. Helfets, R.I. Eglitis, G. Borstel, Comp.Mat.Sci. 29 (2004) 165